Proc. Natl. Acad. Sci. USA
Vol. 74, No. 3, pp. 1028–1031, March 1977
Biochemistry

High-resolution proton magnetic resonance study of the secondary structure of the 3′-terminal 49-nucleotide fragment of 16S rRNA from *Escherichia coli*

(function of S1/cloacin cleavage/thermal stability/GU base-pair)

R. A. BAAN*, C. W. HILBERS†, R. VAN CHARLDORP*, E. VAN LEERDAM*, P. H. VAN KNIPPENBERG*, AND L. BOSCH*

* Department of Biochemistry, State University, Wassenaarseweg 64, Leiden, The Netherlands; and † Department of Biophysical Chemistry, Catholic University, Toernooiveld, Nijmegen, The Netherlands

Communicated by R. G. Shulman, January 10, 1977

ABSTRACT **The 3′ terminus of 16S rRNA has been implicated in the recognition of mRNAs by the ribosome. A fragment containing the 3′-terminal 49 nucleotides cleaved from the rRNA by cloacin DF13 was isolated in a pure form. The secondary structure of this fragment has been studied by measuring the high-resolution proton magnetic resonance spectra. The resonances observed at low field can be assigned to hydrogen-bonded iminoprotons of base-pairs present in the fragment. From the data we conclude that the rRNA fragment, under the conditions used, exists as a hairpin consisting of eight intramolecular base-pairs, the 3′-terminal dodecanucleotide being unpaired. The implications of these findings with respect to the function of the ribosomal protein S1 are discussed.**

One of the most intriguing problems of polypeptide chain initiation is that of the recognition of initiation sites on the messenger. A growing body of evidence exists that the capability to recognize these sites is an inherent property of the ribosome (for a review see ref. 1). More particularly, the 3′ terminus of 16S rRNA has been implicated in the recognition process. Shine and Dalgarno (2) postulated that this 3′ end can base-pair with complementary regions present near the AUG codon in several initiation sites on mRNA. Interestingly, crosslinking (3–5) and other topographic data (6) indicate that various proteins like S1, IF-1, IF-2, IF-3, and S12, which play a role in polypeptide chain initiation, are located in close proximity to the 3′ terminus of 16S rRNA.

Cleavage of the 16S rRNA at a specific site, 49 nucleotides from the 3′-OH terminus, with the bacteriocin cloacin DF13 (7) impairs the ability of the ribosome to respond properly to IF-1 (8). Steitz and Jakes (9) treated a preformed initiation complex containing the isolated A protein initiator region from R17 RNA with colicin E3—known to cleave the 16S rRNA at the same site (10)—and isolated from the complex an RNA·RNA hybrid containing the messenger initiator region and the fragment comprising the 3′-terminal 49 nucleotides of 16S rRNA.

Obviously it would be of great interest to obtain information about the secondary structure of the 3′-terminal part of 16S rRNA. A number of possible secondary foldings can be considered on the basis of the primary structure (Fig. 1). Dahlberg and Dahlberg (6) have proposed that the ribosomal protein S1, which they found to bind to the 3′-terminal dodecanucleotide of 16S rRNA, converts the closed form of Fig. 1*a* or *b* into an open form (Fig. 1*c*), thus allowing for base-pairing with mRNA. We have approached this problem by isolating the 49-nucleotide fragment cleaved from the 16S rRNA by cloacin DF13 (11) and subsequently recording the high-resolution nuclear magnetic resonance (NMR) spectra of the hydrogen-bonded iminoprotons of the base-pairs in this fragment. As has been shown for tRNA (12), individual resonances at low field can be assigned to particular base-pairs by assuming intrinsic positions for the NH protons in AU and GC base-pairs and calculating the upfield shifts introduced by the ring current of the neighboring bases.

Abbreviations: NMR, nuclear magnetic resonance; ppm, parts per million.

MATERIALS AND METHODS

The 3′-terminal 49-nucleotide fragment of 16S rRNA was isolated from 70S ribosomes treated with cloacin DF13, as described (11). The extent of purification was analyzed by electrophoresis on 15% polyacrylamide gels and high pressure liquid chromatography. Furthermore, the latter technique was used for the analysis of the enzymatic digestion products obtained after treatment of the RNA fragment with snake venom phosphodiesterase and T1 RNase.

The secondary structure of the RNA fragment was analyzed by high-resolution NMR spectroscopy. For the NMR experiments a sample was prepared by dissolving the salt-free lyophilized material in 200 μl of an aqueous buffer containing 15 mM Na cacodylate (pH 7.4)/15 mM NaCl/1 mM EDTA. The final concentration of the RNA fragment was about 1.5 mM.

Spectra were obtained with a Bruker 360 MHz NMR spectrometer using the field sweep mode. In order to improve the signal-to-noise ratio, spectra were accumulated in a Nicolet BNC 12 computer for about 1 hr (1000 sweeps) and subsequently cross-correlated (13, 14). The resonance positions expected for the hydrogen-bonded ring NH from each base-pair present in the RNA fragment (based on the structures given in Fig. 1) were calculated from the ring current tables published by Shulman *et al.* (12), modified by Kearns and Wong (15).

The stability of the secondary structure of the RNA fragment was analyzed by recording the NMR spectrum at different temperatures. All resonance positions are referred to the standard reference compound 2,2-dimethyl-2-silapentane-5-sulfonate. To prevent degradation of RNA by contamination with RNase, the usual precautions were taken (11).

RESULTS

Structural integrity of the 3′-terminal fragment

Because it is essential that the Rna fragment is intact and remains so during the measurement of the NMR spectra (about 1 hr at each temperature), we checked the structural integrity before and after the experiments. Various methods were used.

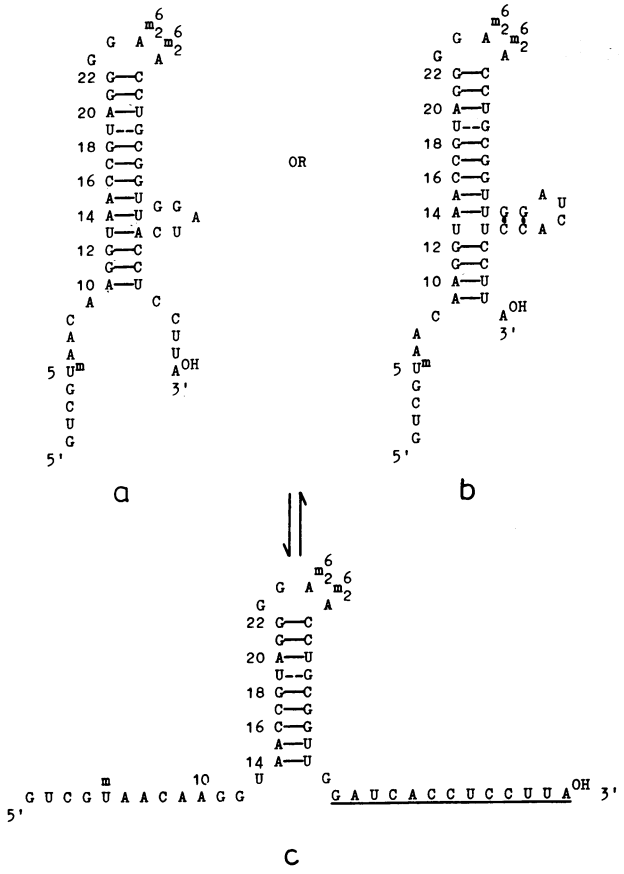

FIG. 1. Alternative structures of the 3′ terminus of 16S rRNA. The fragment represented results from treatment of 70S ribosomes with colicin E3 or cloacin DF13. The numbering of base-pairs corresponds with that in the NMR spectra of Figs. 2 and 3. The sequence underlined is possibly involved in base-pairing with mRNAs.

(*a*) Electrophoresis on 15% polyacrylamide gels containing formamide.
(*b*) High pressure liquid chromatography on Permaphase AAX anion-exchange columns.
(*c*) Digestion with snake venom phosphodiesterase. 3′-Phosphate groups, generated by breakage of the RNA molecule, do not allow complete digestion with this exonuclease.
(*d*) Digestion with spleen phosphodiesterase. Complete digestion does not occur when 5′-phosphates have been generated by breakage. (The intact 49-nucleotide fragment does not contain 5′-terminal phosphate.)
(*e*) Complete digestion with T1 RNase. Analysis of the digest should reveal breaks other than after each guanylic acid residue.
(*f*) Measurement of the ^{31}P NMR spectrum. This procedure was used after the proton NMR measurements. The sample was desalted on Sephadex G-50, converted to the Na^+ form by means of Dowex 50-Na^+, lyophilized, and dissolved in D_2O buffer for ^{31}P resonance measurement.

Optical density patterns obtained with methods *a* and *b* showed homogeneous peaks and virtually no contamination in the higher or lower molecular weight range (see ref. 11). The products of the enzymatic treatments were analyzed by the high-pressure liquid chromatography technique. Complete digestion was reached with both 3′- and 5′-exonuclease. The correct base composition (methods *c* and *d*) or the set of oligonucleotides (method *e*) expected on the basis of the known nucleotide sequence was found.

Finally, the ^{31}P resonance spectrum did not reveal any resonances from 3′- or 5′-monoester phosphates or any resonances from cyclic phosphates.

Table 1. Calculated shifts for the resonance positions of the NH protons in the base-paired region of the 49-nucleotide fragment

Base-pair*		Calculated shift in ppm†
AU	10	0.1
GC	11	0.8
GC	12	0.35
UA	13	0.2
AU	14	1.7
AU	15	0.2
CG	16	0.35
CG	17	1.4
GC	18	0.9
UG	19	—
AU	20	1.2
GC	21	0.8
GC	22	0.95

Intrinsic line positions: AU, −14.5 ppm; GC, −13.6 ppm.
* The numbers refer to the numbering in Figs. 1–3.
† The values are calculated on the basis of the structure given in Fig. 1*a* on the assumption that the base-paired region forms a regular, continuous double helix.

NMR spectra

In Fig. 2*a* the iminoproton spectrum of the fragment recorded at 20° is given. The spectrum consists of nine well-resolved resonances, the line at lowest field being significantly broader than the others. We shall first consider the resonances at −11.5 parts per million (ppm) and −10.7 ppm. These two lines resonate in a spectral region where we do not expect to see resonances from normal Watson-Crick base-pairs. Recently, however, it has been demonstrated that the hydrogen-bonded GN_1H and UN_3H protons of GU pairs resonate in this region (16). The secondary structures proposed for the fragment do indeed indicate the existence of a GU pair (see Fig. 1).

The next step in the analysis of the spectra consists of the prediction of the resonance positions on the basis of the proposed structures and the ring current shift mechanism (see *Materials and Methods*). The ring current shift values and intrinsic positions are given in Table 1.

In Fig. 2*b* the stick spectrum predicted on the basis of the structure in Fig. 1*c* is given. In Fig. 2*c* the stick spectrum of the structure in Fig. 1*a* is shown.

As indicated above, the experimental spectrum contains only nine resonances. Taking each resonance to represent one iminoproton, it is clear that the complete structures as given in Fig. 1*a* and *b*, containing 14 and 15 base-pairs, respectively, are not observed by the NMR method. Therefore we will only compare the spectrum predicted on the basis of Fig. 1*c* with the experimental spectrum.

On the basis of the ring current shift calculations the broadened resonance at −14.2 ppm is assigned to base-pair AU 15. Apparently this resonance is broadened by a fraying reaction at the end of the double helix (17). This being the case, it is to be expected that the resonance coming from AU 14 is broadened beyond the level of detection and therefore it is not indicated in Fig. 2*b*. The resonance positions of the other Watson-Crick base-pairs in the stem are predicted within about 0.1 ppm from the experimental positions.

The fragment was further studied by taking spectra at higher temperatures. These are given in Fig. 3. If the fraying process,

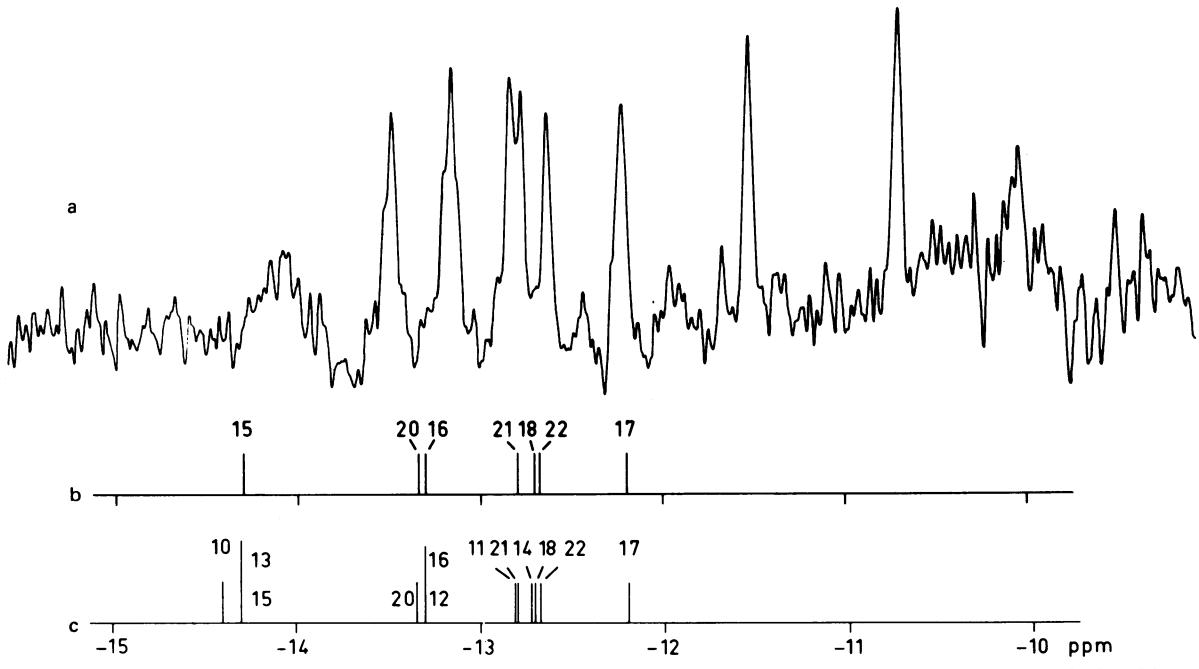

FIG. 2. 360 MHz NMR spectrum of the NH ring protons in the 49-nucleotide fragment. Conditions were as described in *Materials and Methods*. The temperature was 20°. *a*. Experimental spectrum. *b* and *c*. Stick spectra based on the structures given in Fig. 1*c* and *a*, respectively. The resonance line for base-pair AU 14 is omitted in *b* for reasons discussed in the *text*. See Table 1 for the calculated shifts.

mentioned above, proceeds into the stem, one expects the resonance from base-pair CG 16 to melt out. This is indeed confirmed by the experiment. One of the two resonances at lower field, which on the basis of the calculations can either come from CG 16 or from AU 20, starts broadening at 40° and disappears around 50°. At the latter temperature the resonance at −12.1 ppm predicted to come from CG 17 starts to broaden in agreement with expectation. Between 50° and 60° the remaining resonances rather abruptly disappear, indicating that the rest of the double helix melts in an all-or-none process. To check the reversibility of the melting reaction, the sample temperature was subsequently lowered to 25°. The spectrum, originally recorded at this temperature, was recovered.

In an attempt to stabilize the extra base-pairs indicated in Fig. 1*a* and *b* and to be able to distinguish between these two structures, we added Mg^{2+} ions to the sample. The resulting spectrum, recorded at 25°, is given in Fig. 4. This spectrum is identical to that obtained at 25° without Mg^{2+} ions present in solution (see Fig. 3) except for the disappearance of the broad resonance at −14.2 ppm.

DISCUSSION

According to the NMR spectra obtained in the present study it can be concluded that the structure as given in Fig. 1*c* is present in solution up to about 55°. It is somewhat distorted by fraying reactions at the open end of the double helix. Three arguments lead to this conclusion. First, resonances are observed at −11.5 and −10.7 ppm. These are unusual positions for Watson-Crick iminoproton resonances, but they can be assigned to the two iminoprotons present in a GU base-pair (16). Such a base-pair is indeed present in each of the three proposed structures in Fig. 1. Thus, the present results leave little doubt that this feature of the structure exists. Second, the resonance positions predicted on the basis of the structure of Fig. 1*c* and the ring current mechanism reasonably match the experimental spectrum. Although recently improved ring current shift tables have been presented for A′RNA double helices (18), we preferred to use the older values (12). From the analysis of the crystal structure of yeast $tRNA^{Phe}$ it followed that the double-helical parts have a so-called genus type A RNA structure (19), and it is reasonable to expect such a type of double-helical structure for our fragment. In our experience the resonance positions from such helices are better described by the older set of ring current values. Third, these assignments are confirmed by the melting experiments, at least for the resonances that disappear sequentially.

We were not able to detect any resonances from extra double-helical regions of the fragment as proposed in Fig. 1*a* and *b*, even after addition of Mg^{2+} ions. This is not meant to say that these double-helical regions cannot be present for a short period of time. It is, for instance, well known from optical melting experiments performed in conjunction with NMR measurements that the hydrogen-bonded protons may disappear from the NMR spectrum as low as 20° below the optical melting temperature (20). It is, however, safe to say that the lifetime of these extra double-helical regions is shorter than a few milliseconds. This follows from the observation that the resonance from AU 14 is not present in the spectrum and the resonance of AU 15 is already broadened at 20°. Comparison of the predicted with the observed resonance position shows that roughly 6% of the AU 15 base-pairs are disrupted at this temperature and for the solution conditions given in *Materials and Methods*. This amount will of course increase towards the end of the double helix. Mg^{2+} ions are known to stabilize the double-helical state of RNA and DNA molecules. In the present case, however, Mg^{2+} ions appear not to be able to convert the structure in Fig. 1*c* to either that in Fig. 1*a* or that in Fig. 1*b*, at least as seen by NMR. Surprisingly, the resonance from AU 15 even disappears in the presence of Mg^{2+} (Fig. 4). It has been demonstrated that Mg^{2+} ions are able to enhance the exchange of iminoprotons when the double-helical structure becomes disrupted (17). Thus the fraying at the AU 15 position seems not to be reduced by the presence of Mg^{2+} ions. Also, at 5 mM Mg^{2+} the lifetime of the additional base-paired regions pro-

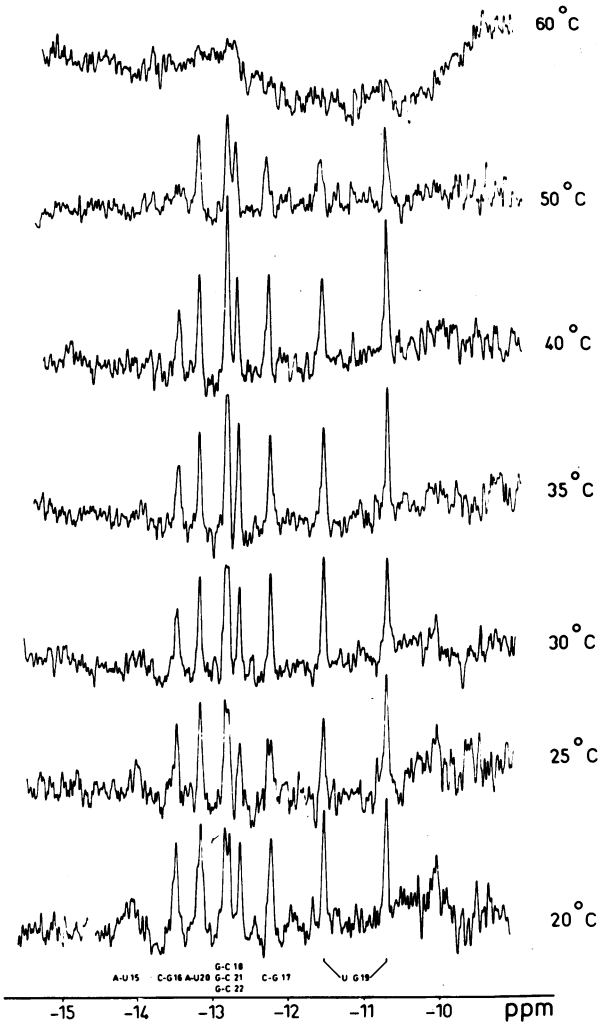

FIG. 3. 360 MHz NMR spectra of the NH ring protons in the 49-nucleotide fragment. Conditions were as described in *Materials and Methods*. The temperature was varied as indicated.

posed in Figs. 1*a* and *b* will be shorter than a few milliseconds. On the basis of these data it is not necessary to invoke a function of ribosomal protein S1 in opening up such regions under physiological conditions (6).

The present results and interpretation are in good agreement with the results of partial T1 RNase digestion of the 49-nucleotide colicin E3 fragment described by Dahlberg and Dahlberg (6). These authors showed that under conditions that G residues do not represent a T1 RNase susceptible site this treatment yielded the oligonucleotide products expected on the basis of the so-called open form of the structure (as drawn in Fig. 1*c*). Identical results were obtained in the presence and absence of S1.

Our results are also in agreement with the evidence from the work of Noller (21). Kethoxal modification of 16S rRNA *in situ* showed that guanylic acid residue 11 (numbering of Fig. 1) is susceptible, at least partially, to this modification. Although information concerning the secondary structure of the intact 16S rRNA *in situ* is lacking, this finding of Noller is consistent

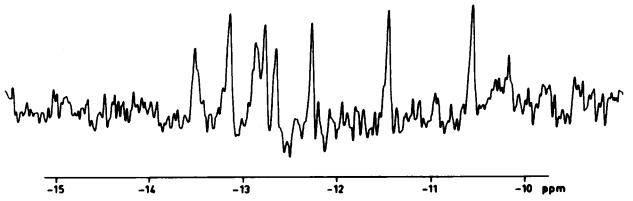

FIG. 4. 360 MHz NMR spectrum of the NH ring protons in the 49-nucleotide fragment. Conditions were as described in *Materials and Methods* except that $MgCl_2$ was present in the sample at 5 mM concentration. The temperature was 25°.

with the open structure presently observed for the isolated fragment.

We thank the Netherlands Organization for the Advancement of Pure Research (ZWO) for support of the high-resolution NMR facility at the University of Groningen and Drs. J. H. van Boom and J. F. M. de Rooij, Department of Organic Chemistry, for their help with the high-pressure liquid chromatography analyses.

1. Bosch, L. (1975) *Proceedings of the 10th FEBS Meeting* (North-Holland Publishing Co., Amsterdam), Vol. 39, pp. 275–295.
2. Shine, J. & Dalgarno, L. (1974) *Proc. Natl. Acad. Sci. USA* **71**, 1342–1346.
3. Kenner, R. A. (1973) *Biochem. Biophys. Res. Commun.* **51**, 932–938.
4. Traut, R. R., Heimark, R. L., Sun, T.-T., Hershey, J. W. B. & Bollen, A. (1974) in *Ribosomes*, eds. Nomura, M., Tissières, A. & Lengyel, P. (Cold Spring Harbor Monograph Series), pp. 271–308.
5. Van Duin, J., Kurland, C. G., Dondon, J. & Grunberg-Manago, M. (1975) *FEBS Lett.* **59**, 287–290.
6. Dahlberg, A. E. & Dahlberg, J. E. (1975) *Proc. Natl. Acad. Sci. USA* **72**, 2940–2944.
7. De Graaf, F. K., Niekus, H. G. D. & Klootwijk, J. (1973) *FEBS Lett.* **35**, 161–165.
8. Baan, R. A., Duijfjes, J. J., Van Leerdam, E., Van Knippenberg, P. H. & Bosch, L. (1976) *Proc. Natl. Acad. Sci. USA* **73**, 702–706.
9. Steitz, J. A. & Jakes, K. (1975) *Proc. Natl. Acad. Sci. USA* **72**, 4734–4738.
10. Samson, A. C. R., Senior, B. W. & Holland, I. B. (1972) *J. Supramol. Struct.* **2**, 135–144.
11. Baan, R. A., Van Charldorp, R., Van Leerdam, E., Van Knippenberg, P. H., Bosch, L., De Rooij, J. F. M. & Van Boom, J. H. (1976) *FEBS Lett.* **71**, 351–355.
12. Shulman, R. G., Hilbers, C. W., Kearns, D. R., Reid, B. R. & Wong, Y. P. (1973) *J. Mol. Biol.* **78**, 57–69.
13. Dadok, J. & Sprecher, R. F. (1974) *J. Magn. Reson.* **13**, 243–248.
14. Gupta, R. K., Becker, E. & Ferretti, J. A. (1974) *J. Magn. Reson.* **13**, 275–290.
15. Kearns, D. R. & Wong, Y. P. (1974) *J. Mol. Biol.* **87**, 755–774.
16. Robillard, G. T., Hilbers, C. W., Reid, B. R., Gangloff, J., Dirheimer, G. & Shulman, R. G. (1976) *Biochemistry* **15**, 1883–1888.
17. Patel, D. J. & Hilbers, C. W. (1975) *Biochemistry* **14**, 2651–2656.
18. Arter, D. B. & Schmidt, P. G. (1976) *Nucleic Acids Res.* **3**, 1437–1447.
19. Sussman, J. L. & Kim, S. H. (1976) *Science* **192**, 853–858.
20. Crothers, D. M., Hilbers, C. W. & Shulman, R. G. (1973) *Proc. Natl. Acad. Sci. USA* **70**, 2899–2901.
21. Noller, H. F. (1974) *Biochemistry* **13**, 4694–4703.